Journal of Alloys and Compounds 501 (2010) 124–129

Contents lists available at ScienceDirect

Journal of Alloys and Compounds

journal homepage: www.elsevier.com/locate/jallcom

Synthesis and luminescent properties of Eu^{3+}-activated molybdate-based novel red-emitting phosphors for white LEDs

An Xie [a,b,*], Ximing Yuan [a,b], Fengxiang Wang [a,b], Yu Shi [c], Jian Li [d], Li Liu [a,b], Zhongfei Mu [e]

[a] Engineering Research Center of Nano-Mineral Materials and Application, Ministry of Education, China University of Geosciences, Wuhan 430074, PR China
[b] Faculty of Materials Science and Chemical Engineering, China University of Geosciences, Wuhan 430074, PR China
[c] School of Environmental Studies, China University of Geosciences, Wuhan 430074, PR China
[d] University of Science and Technology Beijing, Beijing 100083, PR China
[e] Department of Experiment Education, Guangdong University of Technology, Guangzhou 510006, PR China

ARTICLE INFO

Article history:
Received 23 December 2009
Received in revised form 2 April 2010
Accepted 7 April 2010
Available online 18 April 2010

Keywords:
$Na_{0.5}Gd_{0.5}MoO_4$
Li/Na
Red emission phosphor
White LEDs

ABSTRACT

A series of Eu^{3+}-activated molybdate-based phosphors were synthesized. The experimental results indicate that the concentration quenching does not happen in Eu^{3+}-doped $Na_{0.5}Gd_{0.5}MoO_4$ phosphor and the relative emission intensity enhances with the increase of the Eu^{3+} doping ratio, which reaches a maximum at 50 at.% of Eu^{3+}. The emission intensity of $Na_{0.5}Eu_{0.5}MoO_4$ is about 2.26 times higher than that of $Ca_{0.8}MoO_4:Eu_{0.2}{}^{3+}$. The introduction of Li^+ substituting for Na^+ does not change shapes and positions of photoluminescence spectra of $Na_{0.5}Eu_{0.5}MoO_4$ but evidently enhances the emission intensity of Eu^{3+} under 396 nm excitation and the optimal doping concentration of Li^+ is 25 at.%.

1. Introduction

White light-emitting diodes (LEDs) can offer benefits in terms of high luminous efficiency, maintenance, and environmental protection, more and more interest is focused on this solid-state light [1–5]. Presently, the emission bands of LED chips shift to the near-UV range (~400 nm) and the near-UV light can offer higher efficiency solid-state lighting [6–8]. The current commercially applicable red phosphor for UV InGaN-based LEDs is $Y_2O_2S:Eu^{3+}$ [9]; however, the $Y_2O_2S:Eu^{3+}$ red phosphor cannot efficiently absorb in near-UV region and its brightness is about eight times less than that of the blue ($BaMgAl_{10}O_{17}:Eu^{2+}$) and green ($ZnS:(Cu^+, Al^{3+})$) phosphors. In addition, the lifetime of the $Y_2O_2S:Eu^{3+}$ is inadequate under near-UV irradiation for its instability. At present, a great deal of research is being carried out to find a certificated red-emitting phosphor for white LEDs. Yang et al. [10] synthesized a novel red-emitting phosphor $Mg_2GeO_4:Sm^{3+}$ and investigated the properties of luminescence in detail. Fu et al. [11] investigated that the luminescent properties of Eu^{3+}-activated $CaTiO_3$ novel red-emitting phosphors for LEDs. Recently, Liu et al. [12] obtained green light-emitting phase in $Ba_3MgSi_2O_8:Eu^{2+}$, Mn^{2+} full color phosphor for white light-emitting diodes via addition of Si_3N_4. However, the brightness of $Mg_2GeO_4:Sm^{3+}$, $CaTiO_3:Eu^{3+}$ and $Ba_3MgSi_2O_8:Eu^{2+}$, Mn^{2+} are still inadequate for application in white LEDs. Therefore, it is crucial to seek alternative red phosphors with high luminescence and satisfying chemical stability.

In the scheelite-related red phosphors, molybdate is a good choice as a host material. The central Mo^{6+} metal ion is coordinated to four oxygen atoms in tetrahedral symmetry (T_d). Therefore, molybdates are chemically stable, which are better than sulfide and oxysulfide red-emitting phosphors, such as $CaS:Eu^{2+}$, $Y_2O_3:Eu^{3+}$ [13] and $Y_2O_2S:Eu^{3+}$. Moreover, molybdate phosphors have broad and intense absorption bands due to charge transfer (CT) from oxygen to metal in the near-UV region. Scheelite $CaMoO_4$ has almost ideal structure of the $MoO_4{}^{2-}$ and shows excellent thermal and hydrolytic stability. Ci et al. [6] have synthesized the $CaMoO_4:Eu^{3+}$ phosphors and found that the emission intensity of commercial phosphors $Y_2O_2S:Eu^{3+}$ was only 37% of $Ca_{0.80}MoO_4:Eu_{0.20}{}^{3+}$ under 393 nm excitation. However, the brightness of $CaMoO_4:Eu^{3+}$ is still inadequate for application in white LEDs. $CaMoO_4$ host used in red phosphors can be doped with a small quantity of europium, which is 25 mol% at the most, due to the critical concentration for quenching of the Eu^{3+} luminescence in $CaMoO_4$. It is well known that low doping concentrations lead to weak luminescence. Therefore, if the concentration quenching is suppressed, it can be assumed that a large quantity of europium doped into the host lattice can give rise to a high red emission due to the more effective absorption of near-UV light. In addition, it is

* Corresponding author at: Faculty of Materials Science and Chemical Engineering, China University of Geosciences, No. 338 Rumo Road, Hongsan District, Wuhan, Hubei 430074, PR China. Tel.: +86 27 65055955; fax: +86 27 67885201.
E-mail address: whanxie@gmail.com (A. Xie).

0925-8388/$ – see front matter © 2010 Elsevier B.V. All rights reserved.
doi:10.1016/j.jallcom.2010.04.057

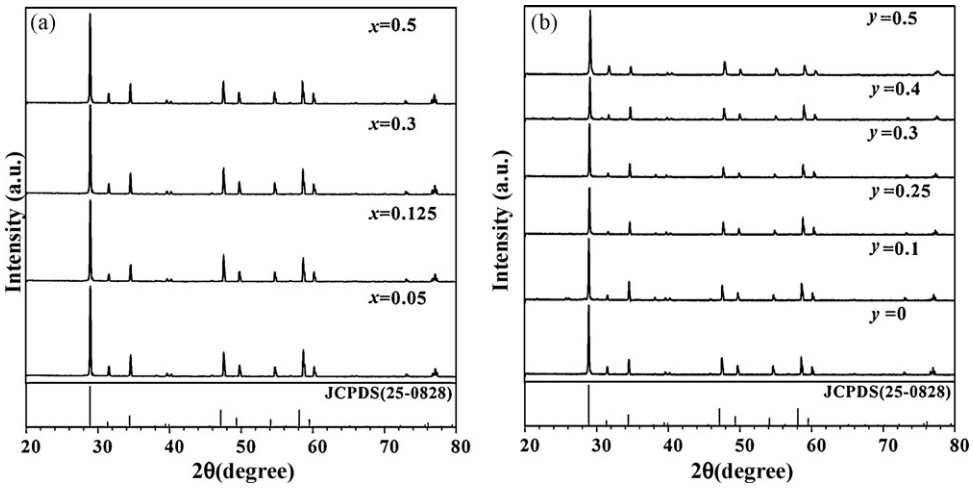

Fig. 1. XRD comparison patterns of (a) $Na_{0.5}Gd_{0.5-x}Eu_xMoO_4$ (x = 0.05, 0.125, 0.30 and 0.50) and (b) $Na_{0.5-y}Li_yEu_{0.5}MoO_4$ (y = 0, 0.10, 0.25, 0.30, 0.40 and 0.50).

well established that the luminescence properties can be tuned by not only the Eu^{3+} concentration but also partial cross-substitution between alkali metals ions. The replacement of Li by Na and/or K is an example [2].

$Na_{0.5}Gd_{0.5}MoO_4$ is similar to $CaMoO_4$ in crystal structure and the MoO_4^{2-} oxyanion complex is the principal constitutive element. In this paper, trivalent europium ion (Eu^{3+})-activated phosphors $Na_{0.5-y}Li_yGd_{0.5-x}Eu_xMoO_4$ were synthesized and their luminescent properties were investigated in detail.

2. Experimental details

The phosphors $Na_{0.5}Gd_{0.5-x}Eu_xMoO_4$ (x = 0.05, 0.10, 0.125, 0.15, 0.20, 0.30, 0.40 and 0.50) and $Na_{0.5-y}Li_yEu_{0.5}MoO_4$ (y = 0.05, 0.10, 0.15, 0.20, 0.25, 0.30, 0.40 and 0.50) were synthesized using solid-state reactions. Stoichiometric amounts of Li_2CO_3 (97%), Na_2CO_3 (99.8%), MoO_3 (99.9%), Gd_2O_3 (99.99%) and Eu_2O_3 (99.99%) were mixed homogeneously in an agate mortar then calcined at 1000 °C for 5 h in air.

The X-ray diffraction (XRD) spectra of these phosphors were identified by a RigakuD/max-II B X-ray diffractometer using Cu as the anode at 40 kV and 100 mA, the X-ray wavelength (λ) was 0.154 178 nm and the lattice parameter of the samples were calculated by MDI Jade 5.0 software.

XRD data for phase identification were collected in a 2θ range from 20° to 80° with a step interval of 0.4°/s. The excitation and emission spectra of these phosphors were recorded with a fluorescence spectrophotometer (Hitachi F-4500) with a 150 W Xe lamp, and the spectral resolution was set up to be 2.5 nm for both the cases of emission and excitation spectra measurement. For the comparison of PLE and PL intensity, the quantity of the phosphor samples has been normalized and measurement conditions (i.e., widths of slit of the excitation and emission monochromators, the PMT detector sensitivity, scan peed) were kept consistent from sample to sample in measurements. Average grain diameters were taken at a JL-1155 Laser particle analyzer (Chengdu Jingxin Powder Analyses Instrument Co., Ltd). The luminescence decay curves were obtained from an Edinburgh FLS920 spectrophotometer. All the measurements were performed at room temperature.

3. Results and discussion

3.1. The analysis of phase characterizations and X-ray structure

Fig. 1a shows the comparison of XRD profiles for $Na_{0.5}Gd_{0.5-x}Eu_xMoO_4$ (x = 0.05, 0.125, 0.30 and 0.50) phase. The diffraction peaks are found to be similar to each other without noticeable shifting. All samples exhibit the same diffraction patterns as appeared in JCPDS card 25-0828 corresponding to the intrinsic diffraction patterns of tetragonal structure of $Na_{0.5}Gd_{0.5}MoO_4$ with space group 141/a (88). No extra-peaks related to the starting materials MoO_3, Eu_2O_3, Gd_2O_3 and Na_2CO_3 are observed. $Na_{0.5}Gd_{0.5}MoO_4$ is similar to $CaMoO_4$ in crystal structure, for the sake of the different valence states and difference of the ion sizes between Na^+ and Eu^{3+}, $Eu^{3+}$is expected to occupy the Gd^{3+} site in this phosphor. The lattice parameters are calculated and shown in Fig. 2a. With the increase of the Eu content, the cell constants and cell volumes increase due to the substitution of Gd^{3+} (ionic radius: r = 0.119 nm when coordination number (CN) = 8) with larger Eu^{3+} (ionic radius: r = 0.121 nm when CN = 8).

The powder XRD patterns of $Na_{0.5-y}Li_yEu_{0.5}MoO_4$ (y = 0, 0.10, 0.25, 0.30, 0.40 and 0.50) are shown in Fig. 1b. According to the JCPDS card 25-0828, all peaks can be indexed with space group 141/a (88). No second phase is observed. Variations of the cell constants caused by different content of Li in the samples are exhibited in Fig. 2b. It is found that with the increase of Li^+ concentration, the unit cell volume and c-axis length gradually decrease, however, the a-axis length has no notable change. The cause lies in the fact that $Na_{0.5}Eu_{0.5}MoO_4$ is similar to $CaMoO_4$ in crystal structure and the central Mo^{6+} metal ion is coordinated by four O^{2-} ions in tetrahedral symmetry (Td). In $Na_{0.5}Eu_{0.5}MoO_4$, the MoO_4^{2-} tetrahedral form layers on the ab plane, and were separated by Na/Eu atoms. On ab plane, the tightly Mo–O bond cannot widely move in the a- and b-axis directions. In the c-axis direction, the layers are loosely connected and separated by Na/Eu atoms. Consequently, the unit cell volume and c-axis length decrease gradually when Li^+ replaces Na^+ step by step. On the other hand, the a-axis length nearly remains unchanged. This is in good agreement with the calculated lattice parameters result shown in Fig. 2b.

Fig. 3 shows the particle size distribution of the $Na_{0.5}Eu_{0.5}MoO_4$ and $Na_{0.25}Li_{0.25}Eu_{0.5}MoO_4$ phosphors. When Li^+ ions are introduced to replace part of Na^+ ions in $Na_{0.5}Eu_{0.5}MoO_4$, the size distribution of the phosphors increases slimly and the average diameter of the particles is 2.28 μm with Li^+ being 25 at.%. The average grain diameter of all samples is less than 2.5 μm and narrow diameter distribution, which is suitable to fabricate the solid-lighting devices [14].

3.2. Luminescent properties of $Na_{0.5}Gd_{0.5-x}MoO_4:Eu_x^{3+}$

The phosphors $Na_{0.5}Gd_{0.5-x}Eu_xMoO_4$ (x = 0.05, 0.10, 0.125, 0.15, 0.20, 0.30, 0.40 and 0.50) with different Eu^{3+}-doped concentration show similar excitation and emission spectra except for their intensities. For the convenience of comparison, only the PLE spectra of phosphors $Na_{0.5}Gd_{0.5-x}Eu_xMoO_4$ (x = 0.05, 0.125 and 0.5) are displayed in Fig. 4. The excitation spectrum for monitoring the $^5D_0 \rightarrow {}^7F_2$ emission (~615 nm) of Eu^{3+} consists of a broad band and some sharp lines. The broad excitation band belongs to a strong charge-transfer band (CTB) of Mo^{6+}–O^{2-} within the MoO_4^{2-} group (λ_{max} ~ 300 nm) at short wavelength from 200 to 360 nm. The charge transfer band (CTB) of Eu^{3+}–O^{2-} keeps the same absorption

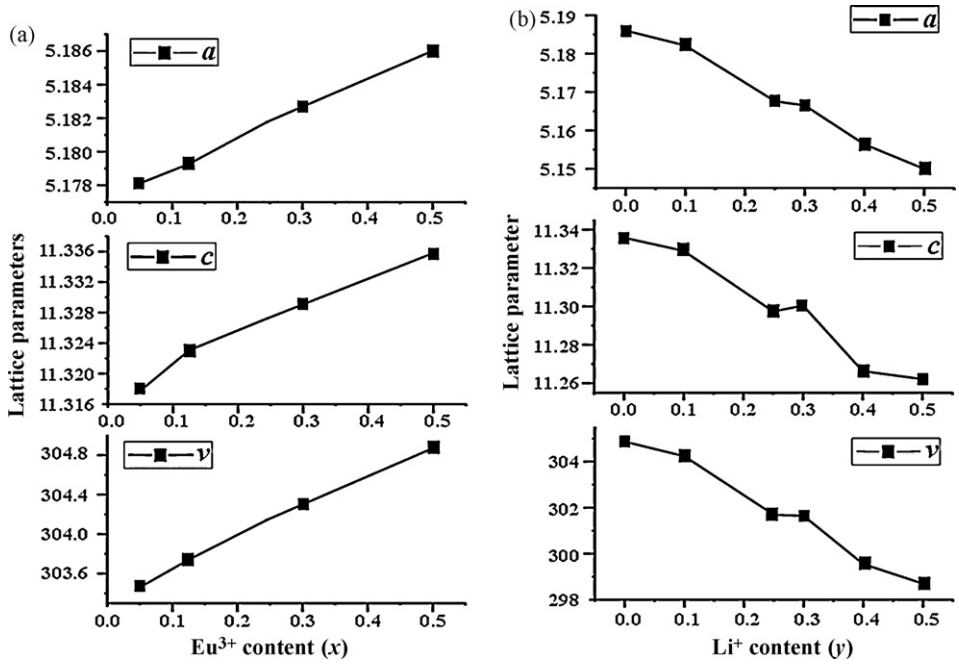

Fig. 2. The calculated lattice parameters of (a) $Na_{0.5}Gd_{0.5-x}Eu_xMoO_4$ (x = 0.05, 0.125, 0.30 and 0.50) and (b) $Na_{0.5-y}Li_yEu_{0.5}MoO_4$ (y = 0, 0.10, 0.25, 0.30, 0.40 and 0.50) (a representation for a-axis length (Å), b representation for b-axis length (Å), v representation for cell volume (Å^3)).

peak at 230 nm when europium atoms have eight-fold coordination in molybdate. $Na_{0.5}Gd_{0.5}MoO_4$ is similar to $CaMoO_4$ in crystal structure, for the sake of the different valence states and ion sizes between Na^+ and Eu^{3+}, $Eu^{3+}$is expected to occupy the Gd^{3+} site in this phosphor. Thus, it is deduced that there is a charge-transfer band (CTB) of Eu^{3+}–O^{2-} at about 230 nm in theory. However, the CT band of Eu^{3+}–O^{2-} is not clearly observed in the excitation spectra, which could be due to possible overlap of the CT band with that of molybdate group. In the range from 360 to 500 nm, all samples show characteristic intra-configurational 4*f*–4*f* emissive transitions of Eu^{3+} from the ground state $^7F_0$ to the excited state $^5L_6$ and $^5D_2$: sharp line $^7F_0 \rightarrow {}^5L_6$ transition for 396 nm and $^7F_0 \rightarrow {}^5D_2$ transition for 466 nm. Compared with the intensity of characteristic absorptions of Eu^{3+} ion in the PLE spectra as shown in Fig. 4, the maximum two absorption of Eu^{3+} $^7F_0 \rightarrow {}^5L_6$ and $^7F_0 \rightarrow {}^5D_2$ peaks become stronger with increasing Eu^{3+} content. However, the intensity of CT absorption of the phosphors $Na_{0.5-x}Eu_xMoO_4$ firstly goes up to its maximum level as the concentration of Eu^{3+} increases to 12.5 at.%; then goes down gradually and does not keep at a stable level until the concentration of Eu^{3+} further exceeds 40 at.%. The experimental results indicate that there is no CT absorption of Gd^{3+}–O^{2-}, when monitored for Eu^{3+} emission (615 nm). In any case, it is a good phenomenon that the phosphors can strongly absorb ultraviolet (396 nm) and visible light (466 nm), which are coupled well with the characteristic emission from UV-LED and blue LED, respectively.

The shape and position of the emission spectra of $Na_{0.5}Gd_{0.5-x}Eu_xMoO_4$ are very similar with each other under 396 and 466 nm excitation, respectively. Fig. 5 displays the composition-dependent PL spectra of $Na_{0.5}Gd_{0.5-x}Eu_xMoO_4$ (x = 0.05, 0.125 and 0.50) under 396 nm excitation. The spectrum essentially consists of sharp lines with wavelengths ranging from 550 to 700 nm. The main emission line is $^5D_0 \rightarrow {}^7F_2$ transition of Eu^{3+} at 615 nm, other transitions from the $^5D_0$

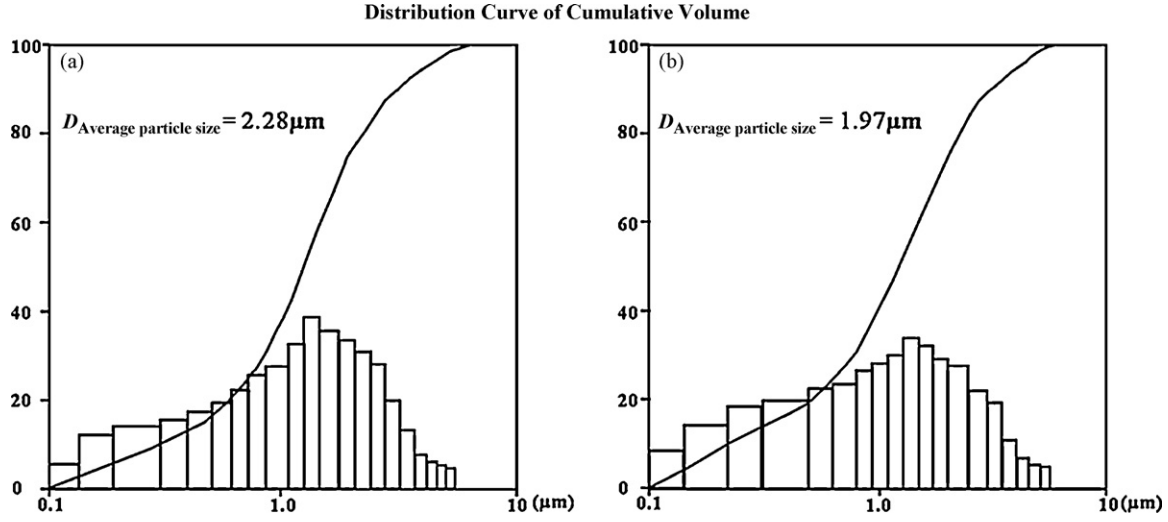

Fig. 3. Particle size distribution of $Na_{0.25}Li_{0.25}Eu_{0.5}MoO_4$ phosphor (curve (a)) and $Na_{0.5}Eu_{0.5}MoO_4$ phosphor (curve (b)), respectively.

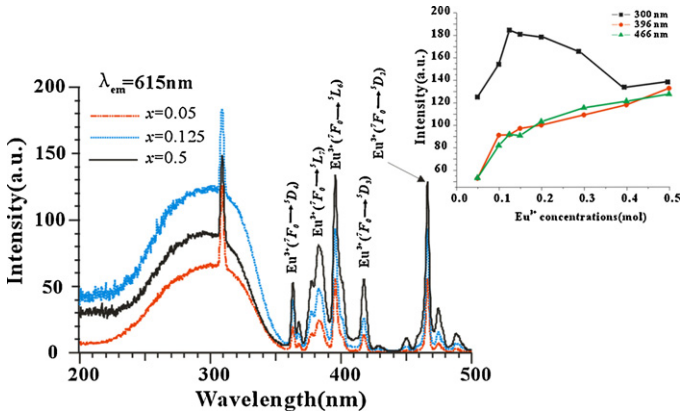

Fig. 4. PLE spectra monitored at 615 nm for phosphors $Na_{0.5}Gd_{0.5-x}Eu_xMoO_4$. The inset figure is the variation of the excitation intensity of the three main peaks with Eu concentration for $Na_{0.5}Gd_{0.5-x}Eu_xMoO_4$ (x = 0.05, 0.10, 0.125, 0.15, 0.20, 0.30, 0.40 and 0.50).

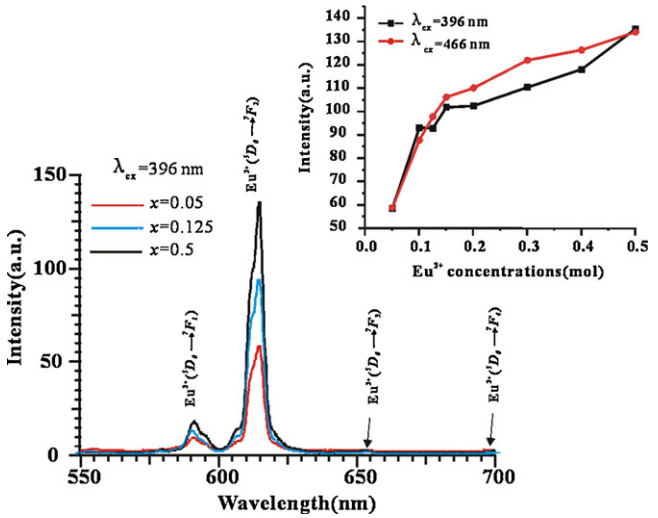

Fig. 5. PL spectra of $Na_{0.5}Gd_{0.5-x}Eu_xMoO_4$ (x = 0.05, 0.125 and 0.50) phosphors under 396 nm near-UV excitation. The inset figure is the variation of the emission intensity with Eu concentration for $Na_{0.5}Gd_{0.5-x}Eu_xMoO_4$ (x = 0.05, 0.10, 0.125, 0.15, 0.20, 0.30, 0.40 and 0.50) under 396 and 466 nm excitation, respectively.

excited levels to ^7F_J (J = 1, 3 and 4) ground states are relatively weak.

Usually the intensity ratio of $^5D_0 \rightarrow {}^7F_2$ to $^5D_0 \rightarrow {}^7F_1$ is regarded as a probe to detect the inversion environmental symmetry around Eu^{3+} in the host. It is known that $^5D_0 \rightarrow {}^7F_2$ electric dipole transition of Eu^{3+} is highly sensitive to its local environment, which appears dominantly only when Eu^{3+} occupies the lattice site of noncentrosymmetric environment in the scheelite phases [15]. The emission peaks at 591 and 615 nm are the magnetic-dipole transition and electric-dipole transition, respectively. The intensity of $^5D_0 \rightarrow {}^7F_2$ (electric-dipole transition) is found to be much stronger than that of $^5D_0 \rightarrow {}^7F_1$ (magnetic-dipole transition) as shown in Fig. 5, which implies that the Eu^{3+} occupies the lattice site of noncentrosymmetric environment in $Na_{0.5}Gd_{0.5-x}Eu_xMoO_4$. Fig. 4 shows an absorption band of a molybdate group in the excitation spectra monitored under 615 nm. However, there is no any emission peak corresponding to MoO_4^{2-} as shown in Fig. 5. It is clearly suggested that the energy absorbed by the MoO_4^{2-} group can be transferred to Eu^{3+} levels nonradiatively.

The effect of the doped Eu^{3+} content in $Na_{0.5}Gd_{0.5-x}Eu_xMoO_4$ (x = 0.05, 0.10, 0.125, 0.15, 0.20, 0.30, 0.40 and 0.50) phosphors on the PL relative intensity at highest $^5D_0 \rightarrow {}^7F_2$ transition of Eu^{3+} at 615 nm is shown in Fig. 5. It can be seen that the luminescence intensity enhances with the increase of the Eu^{3+} doping ratio and reaches a maximum at 50 mol% of Eu^{3+} which means that all the Gd^{3+} is replaced by Eu^{3+}. Zhou et al. [16] synthesized the $Na_{0.5}Gd_{0.5}MoO_4$:Eu^{3+} phosphors and investigated their luminescence properties. The experiment revealed that the luminescence intensity of $Na_{0.5}Gd_{0.5-x}Eu_xMoO_4$ enhanced with the increase of the Eu^{3+} doping ratio and the maximum emission intensity appeared at x = 0.125 compositions. It was also found that concentration quenching happened if the concentration of Eu^{3+} was beyond 0.125. But, our experimental results indicate that concentration quenching does not take place in Eu^{3+}-doped $Na_{0.5}Gd_{0.5}MoO_4$ phosphor. Usually, a low doping ratio gives weak luminescence. Maybe that is why the relative emission intensity of $Na_{0.5}Eu_{0.5}MoO_4$ is much stronger than that of $Na_{0.5}Gd_{0.375}Eu_{0.125}MoO_4$.

$CaMoO_4$:Eu^{3+} is considered as a potential efficient red phosphor that may substitute sulfide phosphors in white LEDs [17–19]. The red phosphor $Ca_{0.80}MoO_4$:$Eu_{0.20}{}^{3+}$ was prepared according to Ci et al. [6]. The relative emission intensity and CIE chromaticity coordinates of $Na_{0.5}Gd_{0.5-x}Eu_xMoO_4$ (x = 0.05, 0.10, 0.125, 0.15, 0.20, 0.30, 0.40 and 0.50) and $Ca_{0.80}MoO_4$:$Eu_{0.20}{}^{3+}$ were calculated and listed in Table 1. When the excitation wavelength is 396 nm, the emission intensity of $Na_{0.5}Eu_{0.5}MoO_4$ is about 2.26 times higher than that of $Ca_{0.80}MoO_4$:$Eu_{0.20}{}^{3+}$.

3.3. *Influence of the replacement of Na by Li on luminescent properties of $Na_{0.5}Eu_{0.5}MoO_4$*

In order to improve the relative emission intensity of the $Na_{0.5}Eu_{0.5}MoO_4$, Na^+ was partial replaced by Li^+. The shapes and positions of excited and emissive spectra of $Na_{0.5-y}Li_yEu_{0.5}MoO_4$ (y = 0.05, 0.10, 0.15, 0.20, 0.25, 0.30, 0.40 and 0.50) do not change with the difference of Li^+ concentration.

However, the relative emission intensity changes evidently. The relative emission intensities of $Na_{0.5-y}Li_yEu_{0.5}MoO_4$ are listed in Table 1. It can be concluded that the relative intensities of the phosphors can be divided into two stages because of the different doping concentrations of Li^+. At the first stage, the luminescence intensity increases with increasing content of Li^+ and reaches the maximum when Li^+ doping amount is 25 at.%; at the second stage, the relative intensity reduces when the concentration of Li^+ is higher than 25 at.%.

$Na_{0.5-y}Li_yEu_{0.5}MoO_4$ is similar to $CaMoO_4$ in crystal structure and the MoO_4^{2-} oxyanion complex is the principal constitutive element. For $Na_{0.5-y}Li_yEu_{0.5}MoO_4$, the Li^+ or Na^+ mixed with Eu^{3+} randomly occupies the Ca^{2+} sites. The calculated lattice parameters result of $Na_{0.5-y}Li_yEu_{0.5}MoO_4$ shows the unit cell volume and c-axis length decrease gradually and the a-axis length nearly remains unchanged when Li^+ replaces Na^+ step by step. Thus, it is deduced that the Eu^{3+}–O^{2-} distance may become shorter, which could be attributed to the smaller size of Li^+ as compared to that of Na^+. Consequently, with the introducing appropriate Li^+ content, the emerged short Eu^{3+}–O^{2-} distance increases the probability for the exchange interaction to occur that results in improving the luminescence intensity of phosphor $Na_{0.5}Eu_{0.5}MoO_4$. In addition, the result shows that the small amount of Li^+ alter the sublattice surrounding field around Eu^{3+} ions and make them far away in inversion symmetry in $Na_{0.5}Eu_{0.5}MoO_4$. Generally, the 4f orbit of Eu^{3+} is shielded by the outside $5S^2$ and $5P^6$ orbits. When the Eu^{3+} ions occupy the lattice sites without inversion symmetry, the limit of f–f transitions of Eu^{3+} may be relaxed [20]. Therefore, besides the emerged short Eu^{3+}–O^{2-} distance increases, another possible factor which might contribute to improvement of luminescence intensity is the relaxation of f–f transitions of Eu^{3+} by

Table 1
Comparison of CIE chromaticity coordinates and $^5D_0 \rightarrow {}^7F_2$ relative emission intensity of $Na_{0.5-y}Li_yGd_{0.5-x}Eu_xMoO_4$ ($0.05 \le x \le 0.50$; $0.05 \le x \le 0.50$) and $Ca_{0.80}MoO_4:Eu_{0.20}^{3+}$ (λ_{ex} = 396 nm).

Phosphors	CIE chromaticity coordinates[a]		$^5D_0 \rightarrow {}^7F_2$ relative intensity[b]
	x	*y*	
$Ca_{0.8}MoO_4:Eu_{0.2}^{3+}$	**0.645**	**0.355**	**1.00**
$Na_{0.5}Gd_{0.45}Eu_{0.05}MoO_4$	0.621	0.379	0.97
$Na_{0.5}Gd_{0.4}Eu_{0.1}MoO_4$	0.636	0.364	1.55
$Na_{0.5}Gd_{0.375}Eu_{0.125}MoO_4$	0.635	0.364	1.55
$Na_{0.5}Gd_{0.35}Eu_{0.15}MoO_4$	0.636	0.363	1.70
$Na_{0.5}Gd_{0.3}Eu_{0.2}MoO_4$	0.636	0.364	1.71
$Na_{0.5}Gd_{0.2}Eu_{0.3}MoO_4$	0.638	0.361	1.84
$Na_{0.5}Gd_{0.1}Eu_{0.4}MoO_4$	0.637	0.362	1.97
$Na_{0.5}Eu_{0.5}MoO_4$	**0.646**	**0.354**	**2.26**
$Na_{0.45}Li_{0.05}Eu_{0.5}MoO_4$	0.644	0.356	2.52
$Na_{0.4}Li_{0.1}Eu_{0.5}MoO_4$	0.645	0.354	2.69
$Na_{0.35}Li_{0.15}Eu_{0.5}MoO_4$	0.648	0.352	2.77
$Na_{0.3}Li_{0.2}Eu_{0.2}MoO_4$	0.651	0.349	2.81
$Na_{0.25}Li_{0.25}Eu_{0.5}MoO_4$	**0.654**	**0.346**	**3.10**
$Na_{0.2}Li_{0.3}Eu_{0.5}MoO_4$	0.651	0.349	2.90
$Na_{0.1}Li_{0.4}Eu_{0.5}MoO_4$	0.650	0.350	2.78
$Li_{0.5}Eu_{0.5}MoO_4$	0.648	0.352	2.11

[a] The NTSC standard values *x* = 0.670 and *y* = 0.330.
[b] The intensity of $Ca_{0.8}MoO_4:Eu_{0.2}^{3+}$ is regarded as 1.00.

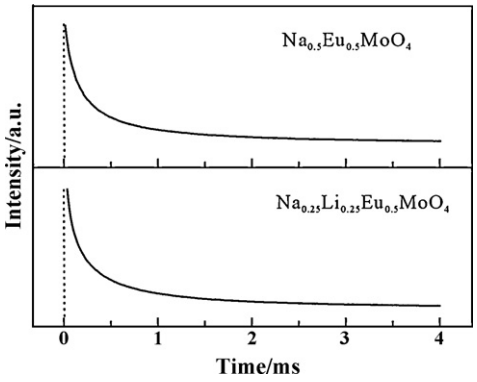

Fig. 6. Photoluminescence decay curve of Eu^{3+} in $Na_{0.5-y}Li_yEu_{0.5}MoO_4$ (y = 0, 0.25) (excited at 396 nm, monitored at 615 nm).

doping appropriate amount of Li^+. The luminescence intensity of $Na_{0.5}Eu_{0.5}MoO_4$ will decrease with the addition of superfluous amount of Li^+, which results in changing the Eu atomic location and causing lattice distortion. And the optimum concentration of Li^+ in $Na_{0.5-y}Li_yEu_{0.5}MoO_4$ phosphors is 25 at.%.

The chromaticity coordinates of the phosphor $Na_{0.5-y}Li_yEu_{0.5}MoO_4$ (λ_{ex} = 396 nm) were calculated and listed in Table 1. The chromaticity coordinates of the phosphor $Na_{0.25}Li_{0.25}Eu_{0.5}MoO_4$ are x = 0.654, y = 0.346, which are closer to the standard of National Television System Committee (NTSC) (x = 0.670, y = 0.330) than those of $Na_{0.5}Eu_{0.5}MoO_4$ (x = 0.646, y = 0.354). The result indicates that appropriate Li^+ replacing Na^+ not only enhances the relative intensity but also improves the color purity of the red-emitting phosphor.

The decay curves for $^5D_0 \rightarrow {}^7F_2$ (615 nm) of the Eu^{3+} in the phosphors $Na_{0.5-y}Li_yEu_{0.5}MoO_4$ (y = 0, 0.25) are shown in Fig. 6. They are well fitted with a single-exponential function as $I = I_0 \exp(-t/\tau)$, and the lifetime τ values for $Na_{0.5}Eu_{0.5}MoO_4$ and $Na_{0.25}Li_{0.25}Eu_{0.5}MoO_4$ are 0.397 and 0.436 ms, respectively. With the introducing appropriate Li^+ content, the samples lifetime τ values increase.

4. Conclusions

The phosphors $Na_{0.5}Gd_{0.5-x}Eu_xMoO_4$ (x = 0.05, 0.10, 0.125, 0.15, 0.20, 0.30, 0.40 and 0.50) and $Na_{0.5-y}Li_yEu_{0.5}MoO_4$ (y = 0.05, 0.10, 0.15, 0.20, 0.25, 0.30, 0.40 and 0.50) were synthesized using solid-state reactions. The experimental results indicate that concentration quenching does not happen in Eu^{3+}-doped $Na_{0.5}Gd_{0.5}MoO_4$ phosphor and the relative emission intensity enhances with the increase of the Eu^{3+} doping ratio and reaches a maximum at 50 at.% of Eu^{3+}. The emission intensity of $Na_{0.5}Eu_{0.5}MoO_4$ is about 2.26 times higher than that of $Ca_{0.8}MoO_4:Eu_{0.2}^{3+}$.

Appropriate amount of Li^+ is introduced into $Na_{0.5}Eu_{0.5}MoO_4$ to substitute Na^+, the intensities of emission can be evidently improved. The emission intensity ($^5D_0 \rightarrow {}^7F_2$) is enhanced by 3.10 times and the chromaticity coordinates (x = 0.654, y = 0.346) are closer to the NTSC standard values (x = 0.670, y = 0.330) than that of $Ca_{0.8}MoO_4:Eu_{0.2}^{3+}$ (x = 0.645, y = 0.355) when Li^+ doping concentration is 25 at.%. Furthermore, the analysis of the experimental results suggest that besides the emerged short Eu^{3+}–O^{2-} distance increases, another possible factor which might contribute to improvement of luminescence intensity of $Na_{0.5-y}Li_yEu_{0.5}MoO_4$ is the relaxation of *f*–*f* transitions of Eu^{3+} by doping appropriate amount of Li^+. All the results indicate that the red phosphor is a suitable candidate of red-emitting phosphor for the fabrication of white LEDs.

Acknowledgment

We acknowledge generous financial support from the Major Science and Technology Projects of Wuhan City Science and Technology Bureau (No. 200810321148).

References

[1] Y. Hu, W. Zhuang, H. Ye, D. Wang, S. Zhang, X. Huang, J. Alloys Compd. 390 (2005) 226–229.
[2] Z.L. Wang, H.B. Liang, L.Y. Zhou, H. Wu, M.L. Gong, Q. Su, Chem. Phys. Lett. 412 (2005) 313–316.
[3] S. Yan, J. Zhang, X. Zhang, S. Lu, X. Ren, Z. Nie, X. Wang, J. Phys. Chem. C 111 (2007) 13256–13260.
[4] J.G. Wang, X.P. Jing, C.H. Yan, J.H. Lin, J. Electrochem. Soc. 152 (2005) G186–G188.
[5] A. Xie, X.M. Yuan, J.J. Wang, F. Wang, Sci. China Ser. E-Technol. Sci. 52 (2009) 1913–1918.
[6] Z. Ci, Y. Wang, J. Zhang, Y. Sun, Physica B 403 (2008) 670–674.
[7] A. Xie, X.M. Yuan, S.J. Hai, J.J. Wang, F.X. Wang, L. Li, J. Phys. D: Appl. Phys. 42 (2009) 1–7.
[8] Z.C. Wu, J.X. Shi, J. Wang, M.L. Gong, Q. Su, J. Solid State Chem. 179 (2006) 2356–2360.

[9] S. Neeraj, N. Kijima, A.K. Cheetham, Chem. Phys. Lett. 387 (2004) 2–6.
[10] H.M. Yang, Z.L. Wang, M.L. Gong, H.B. Liang, J. Alloys Compd. 488 (2009) 331–333.
[11] J.P. Fu, Q.H. Zhang, Y.G. Li, H.Z. Wang, J. Alloys Compd. 485 (2009) 418–421.
[12] Y.H. Liu, Z.Y. Mao, W.H. Yu, Q.F. Lu, D.J. Wang, J. Alloys Compd. 493 (2010) 406–409.
[13] L. Muresan, E.J. Popovici, F. Imre-Lucaci, R. Grecu, E. Indrea, J. Alloys Compd. 483 (2009) 346–349.
[14] R.P. Rao, J. Electrochem. Soc. 143 (1996) 189–197.
[15] A. Kato, S. Oishi, T. Shishido, M. Yamazaki, S. Iida, J. Phys. Chem. Solids 66 (2005) 2079–2081.
[16] L.Y. Zhou, L.H. Yi, R.F. Sun, F.Z. Gong, J.H. Sun, J. Am. Ceram. Soc. 91 (2008) 3416–3418.
[17] X. Li, Z.P. Yang, L. Guan, J. Synth. Cryst. 36 (2007) 1192–1196.
[18] J. Liu, H.Z. Lian, C.S. Shi, Opt. Mater. 29 (2007) 1591–1594.
[19] Z. Wang, H. Liang, M. Gong, Q. Su, Opt. Mater. 29 (2006) 896–900.
[20] G. Blasse, B.C. Grabmaier, Luminescent Materials, Spinger, Berlin and Heidelberg, 1994.